

## Supporting Information

### **Metal-organic framework-encapsulated nanoparticles for synergetic chemo/chemo-dynamic therapy with targeted H<sub>2</sub>O<sub>2</sub> self-supplying**

*Ruixue Cui,<sup>a</sup> Jing Shi,<sup>a</sup> and Zhiliang Liu\*<sup>a</sup>*

<sup>a</sup>Inner Mongolia Key Laboratory of Chemistry and Physics of Rare Earth Materials, School of Chemistry and Chemical Engineering, Inner Mongolia University, Hohhot 010000, P.R. China

E-mail: cezlliu@imu.edu.cn. Fax/Tel: +86-471-4994375 (Prof. Z. Liu)

### Content

Figure S1. a) PXRD spectra of CaO<sub>2</sub> nanoparticles; b) PXRD spectra of CaO<sub>2</sub> nanoparticles, CZ, CDZ, and CDZH nanohybrids.

Figure S2. a) TEM image of CaO<sub>2</sub> nanoparticles; b) HRTEM image of CaO<sub>2</sub> nanoparticles (A, B, C: the SAED pattern of CaO<sub>2</sub> nanoparticles).

Figure S3. The SEM images of Cu/ZIF-8 nanoparticles at different magnifications.

Figure S4. The FTIR curve of DOX, HA, Cu/ZIF-8 nanoparticles and CDZH nanohybrids.

Figure S5. High-resolution XPS spectra of C 1s (a), N 1s (b), and Zn 2p (c) in CDZH nanohybrids.

Figure S6. The TGA curve of CaO<sub>2</sub> nanoparticles, Cu/ZIF-8 nanoparticles, CDZ and CDZH nanoplateforms.

Figure S7. The fluorescence spectra of CDZH and DOX (Ex=470 nm).

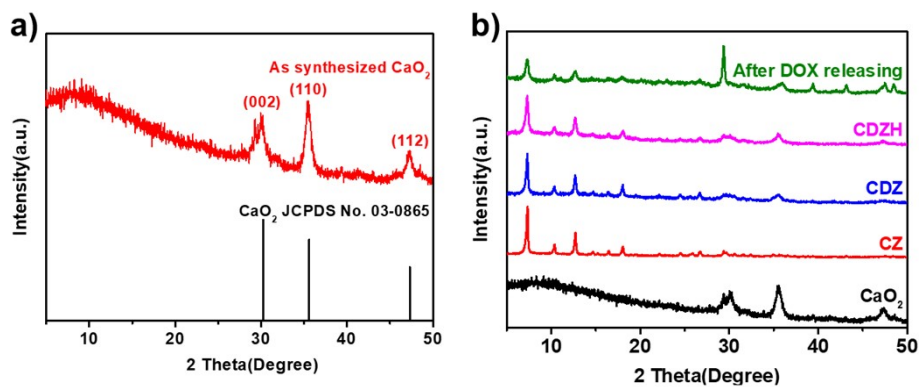
Figure S8. a) The UV-vis spectra of the supernatant of CDZH; b) The UV-vis spectra of calibration curve of DOX.

Figure S9. ESR spectra of CDZH at different pH values with 5,5-dimethyl-1-pyrroline N-oxide (DMPO) as the spin trap at pH=7.4 (a), 6.5 (b), and 5.6(c).

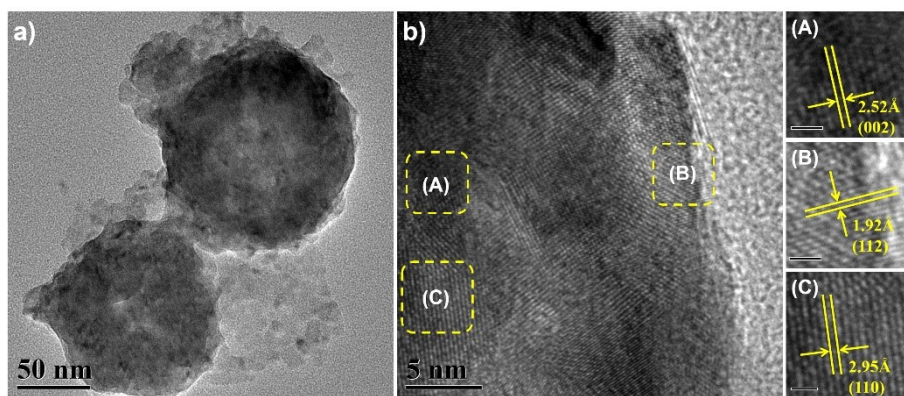
Figure S10. Oxygen concentration of PBS buffer solution with pH 5.6(a), 7.4(b), and 8.0(c) after adding CDZH (water was used as the control).

Figure S11. a) Viabilities of HL-7702 cells cultured with CaO<sub>2</sub> (black) and DOX (red) evaluated by MTT; b) Viabilities of A549 cells cultured with CaO<sub>2</sub> (black) and DOX

(red) evaluated by MTT.



**Figure S1.** a) XRD spectra of CaO<sub>2</sub> nanoparticles; b) XRD spectra of CaO<sub>2</sub> nanoparticles, CZ, CDZ, and CDZH nanohybrids.



**Figure S2.** a). TEM image of CaO<sub>2</sub> nanoparticles; b). HRTEM image of CaO<sub>2</sub> nanoparticles (A, B, C: the SAED pattern of CaO<sub>2</sub> nanoparticles).

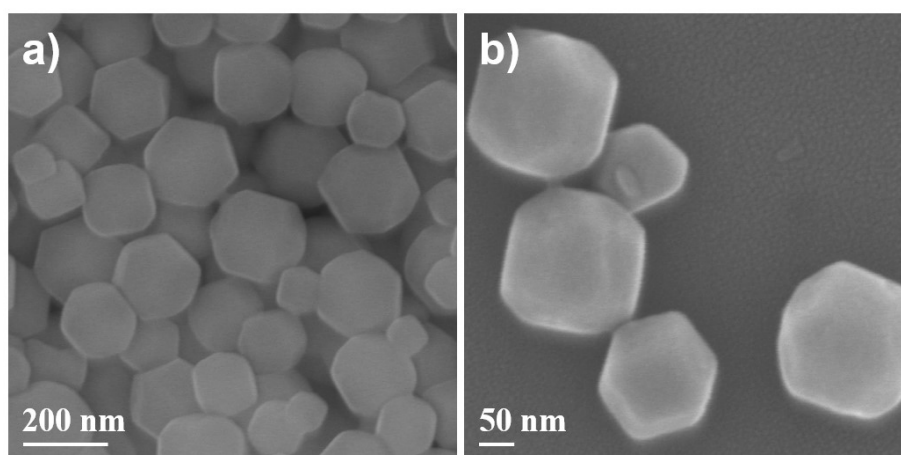


**Figure S3.** The SEM images of Cu/ZIF-8 nanoparticles at different magnifications.

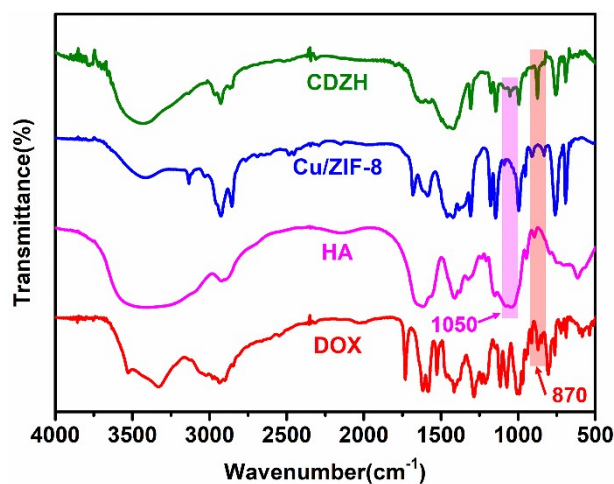


**Figure S4.** The FTIR curve of DOX, HA, Cu/ZIF-8 nanoparticles and CDZH nano hybrids.

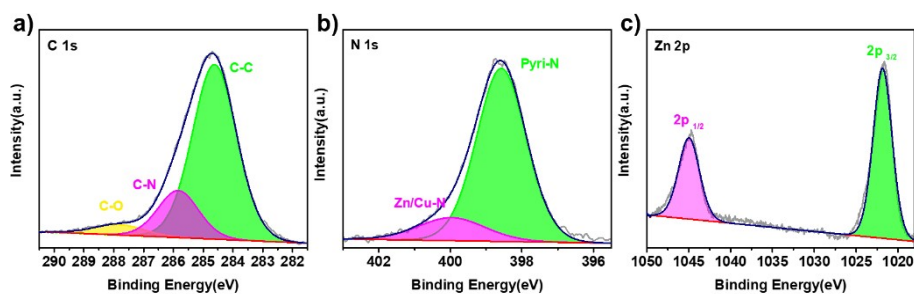


**Figure S5.** High-resolution XPS spectra of C 1s (a), N 1s (b), and Zn 2p (c) in CDZH nano hybrids.

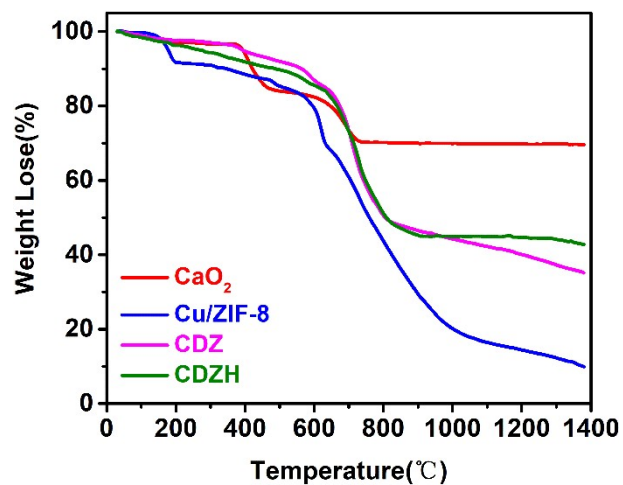


**Figure S6.** The TGA curve of  $\text{CaO}_2$  nanoparticles, Cu/ZIF-8 nanoparticles, CDZ and CDZH nano platforms.

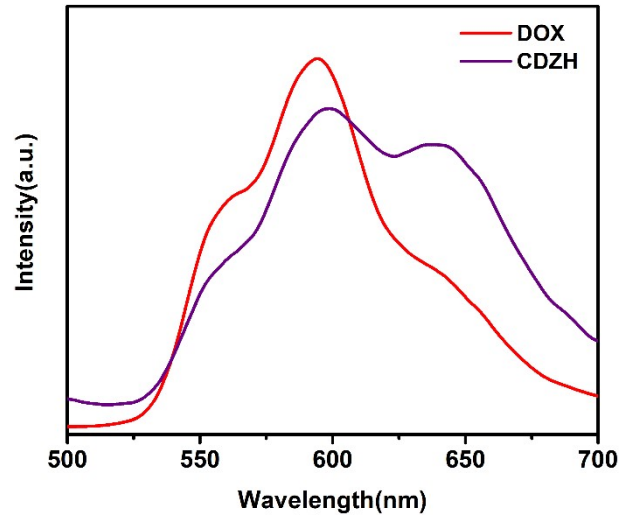


Figure S7. The fluorescence spectra of CDZH and DOX (Ex=470 nm).

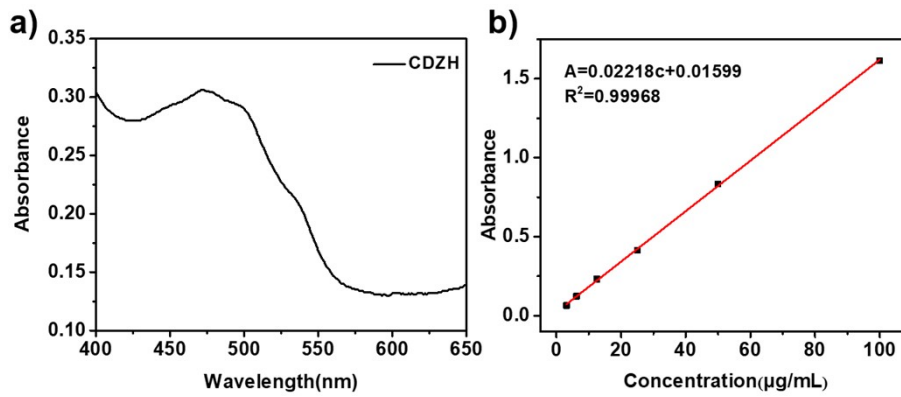


Figure S8. a) The UV-vis spectra of the supernatant of CDZH; b) The UV-vis spectra of calibration curve of DOX.

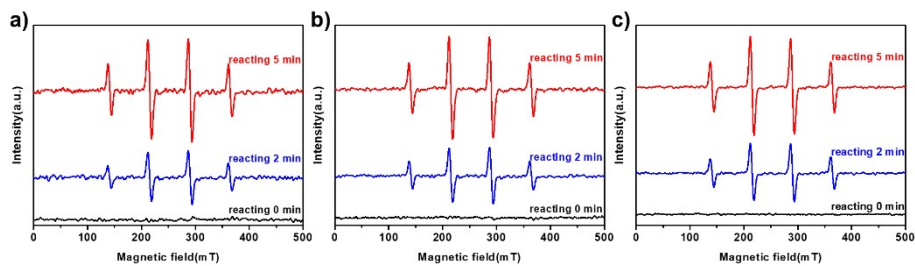
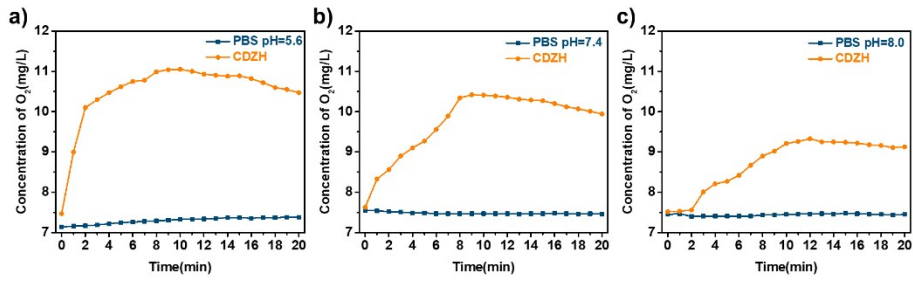
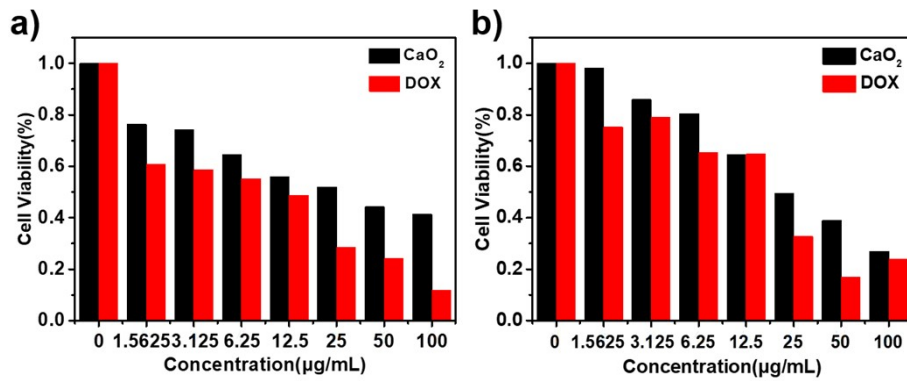


Figure S9. ESR spectra of CDZH at different pH values with 5,5-dimethyl-1-pyrroline N-oxide (DMPO) as the spin trap at pH=7.4 (a), 6.5 (b), and 5.6(c).



**Figure S10.** Oxygen concentration of PBS buffer solution with pH 5.6(a), 7.4(b), and 8.0(c) after adding CDZH (water was used as the control).



**Figure S11.** a) Viabilities of HL-7702 cells cultured with CaO<sub>2</sub> (black) and DOX (red) evaluated by MTT; b) Viabilities of A549 cells cultured with CaO<sub>2</sub> (black) and DOX (red) evaluated by MTT.